DOI 10.1590/s1982-21702024000100006

SPECIAL SECTION - Brazilian Colloquiums on Geodetic Sciences

XII Colóquio Brasileiro de Ciências Geodésicas
V Simpósio Brasileiro de Geomática

OBTAINING THE OCEAN TIDE FROM GNSS POSITIONING ALLIED TO DATA FILTERING METHODS

Valder Alvaro da Luz Silva[1] - ORCID: 0009-0007-9902-6698

Daniele Barroca Marra Alves[1] - ORCID: 0000-0002-9033-8499

Paulo T. Setti Jr.[2] - ORCID: 0000-0001-5080-1832

Felipe Rodrigues Santana[3] - ORCID: 0000-0001-6410-7999

[1]Universidade Estadual Paulista (UNESP), Departamento de Cartografia, Presidente Prudente - São Paulo, Brasil.
E-mail: valder_alvaro@hotmail.com.br; daniele.barroca@unesp.br

[2]University of Luxembourg, Faculty of Science, Technology and Medicine, Esch-sur-Alzette, Luxembourg.
E-mail: paulo.setti@uni.lu

[3]Universidade Federal do Paraná, Programa de Pós-Graduação Ciências Geodésicas, Curitiba, Brasil.
E-mail: felipesantana33@gmail.com

Received in 30th July 2023.
Accepted in 04th March 2024.

Abstract:

The evolution of Global Navigation Satellite System (GNSS) positioning has greatly benefited several areas of knowledge. For Hydrography, an application improved by this science is the measurement of sea level oscillations resulting from tides. However, to satisfactorily retrieve this information, it is necessary to use low-pass filters (LPF) to match high frequency signals resulting from variation of the vertical component of the GNSS positioning to those of low frequency that characterizes tidal waves. Currently, there is a wide variety of LPF, which are selected according to the required purpose. Thus, the objective of this study is to obtain tidal height variations with high accuracy by applying LPF in GNSS positioning vertical coordinates tracked by an onboard GNSS receiver. For this purpose, field research and the processing of obtained data was performed. Then, two data filters were tested: the Simple Moving Average (SMA) Filter and wavelet compression. In both options, the results reached centimetric accuracy when compared to the real tide in the region of study. However, through quantitative and qualitative evaluations, it was verified that the SMA filter was considered more advantageous because, in addition to its high accuracy, it has a simpler application and less expensive in computational terms.

Keywords: Tides; Positioning; GNSS; PPK; SMA Filter; Wavelet.

How to cite this article: SILVA VAL, ALVES DBM, SETTI JR. PT, SANTANA FR. Obtaining the ocean tide from GNSS positioning allied to data filtering methods. *Bulletin of Geodetic Sciences*. 30: e2024006, 2024.

1. Introduction

The intense development of GNSS positioning, as well as the increasing improvement of its accuracy, has influenced several areas of knowledge nowadays. Hydrography is one of these areas, which, in addition to directly using GNSS positioning to measure depths on nautical charts (IHO, 2005), also looks for an indirect way of applying this technique, aiming at efficiency in carrying out activities such as tidal studies and measurements.

The variation of sea level caused by astronomical tides is an extremely important factor in the hydrographic context. Tides are essential in bathymetric data processing to determine the precise depth of a surveyed area (Ismail et al., 2022). Furthermore, the vertical reference of the depths included in all produced nautical charts depends on its analysis. A bulletin from the United States Army Corps of Engineers (USACE) stated that this has been one of the main reasons for disagreements and disapproval of updating charts after dredging activities (USACE, 2013). Thus, it is verified that the reliability of these cartographic documents is deeply connected to adequate measurement and study of tides.

In this sense, GNSS positioning comes up as a more advantageous option when compared to conventional methods of tidal data measurements, using tide gauges fixed to the shore. The distance between these devices and the surveying vessel causes systematic errors resulted from the difference in location (Chang et al., 2002; Mann, 2007). To mitigate these errors, some studies have been conducted using GNSS receivers dedicated to acquiring tidal measurements fixed in mobile platforms performing hydrographic survey, generating results with greater accuracy, when treated appropriately (Deloach, 1996; Bouin et al., 2009; Oliveira Jr. et al., 2010).

For this purpose, digital data filters emerge as a valuable tool. Its use in digital signal processing began in the 1960s and 1970s, with the availability of the first computers, being applied primarily for military purposes, oil exploration, space exploration and medical imaging (Smith, 1999). The filters range from the simplest, such as the Simple Moving Average Filter, which uses the moving average concept, to the most complex ones, such as those that use orthogonal filters banks generated by Discrete Wavelet Transform (DWT), (Graps, 1995). In all these cases, filters are used to treat signals obtained by sensors, making them suitable for certain applications; it is in this sense that Hydrography can benefit from the use of these filters applied to GNSS positioning data to obtain tidal measurements.

To contribute to this theme, the present work aims to apply and evaluate a methodology to retrieve tidal information, using an on-board GNSS receiver to collect observations. In addition, the research also focuses on finding the best way to perform the post-processing of the positioning results, comparing different data filters to remove high frequency signals. This attenuation concerned with generating the least possible loss of data and providing the greatest similarity with the reference signal, showing the feasibility of obtaining high-accuracy tidal information through the procedures presented.

2. Relative GNSS Positioning

Relative GNSS positioning is the method in which an unknown position is estimated based on another with known coordinates. In this mode, basically, the double-differences (DD) of carrier phase, pseudodistances or both are used as observables (Odijk, 2017).

The DD depend exclusively on the simultaneity of the observations obtained by at least two receivers, tracking signals from the same satellites. This configuration allows the elimination of satellite and receiver clock errors, as well as the significant mitigation of neutral atmosphere and ionospheric effects when short baselines are employed (Langley et al., 2017).

In case one of the receivers keeps moving, acquiring data from a certain path, the relative positioning is classified as kinematic. This is divided into Real-Time Kinematic (RTK), when the coordinates are corrected as they are collected, and Post-Processed Kinematic (PPK), when data from GNSS observations from both stations and the ephemeris of the satellite constellations are later used to estimate the coordinates (Everett et al., 2022).

Regarding the quality of the positioning method, when carrier phase DD are used and the integer value of the ambiguities are estimated, the relative method can achieve a few centimeters of accuracy (Odijk and Wanninger, 2017). This fact makes it to be employed in a wide range of applications, which include the remote measurement of natural phenomena, such as the astronomical tide.

3 Tides

The tide is the sea level variation under the influence of astronomical forces. Primarily, this movement is the result of the action of the gravitational attraction between the Earth and the Moon, as well as the centrifugal force produced by the rotation of the planet around the center of mass of the Earth-Moon system (Franco, 2009), as illustrated in Figure 1. The effect generated is the accumulation of water mass in the direction of the vectors resulting from these forces, which accompanies the realization of the lunar orbital movement with a period of about 27,3 days.

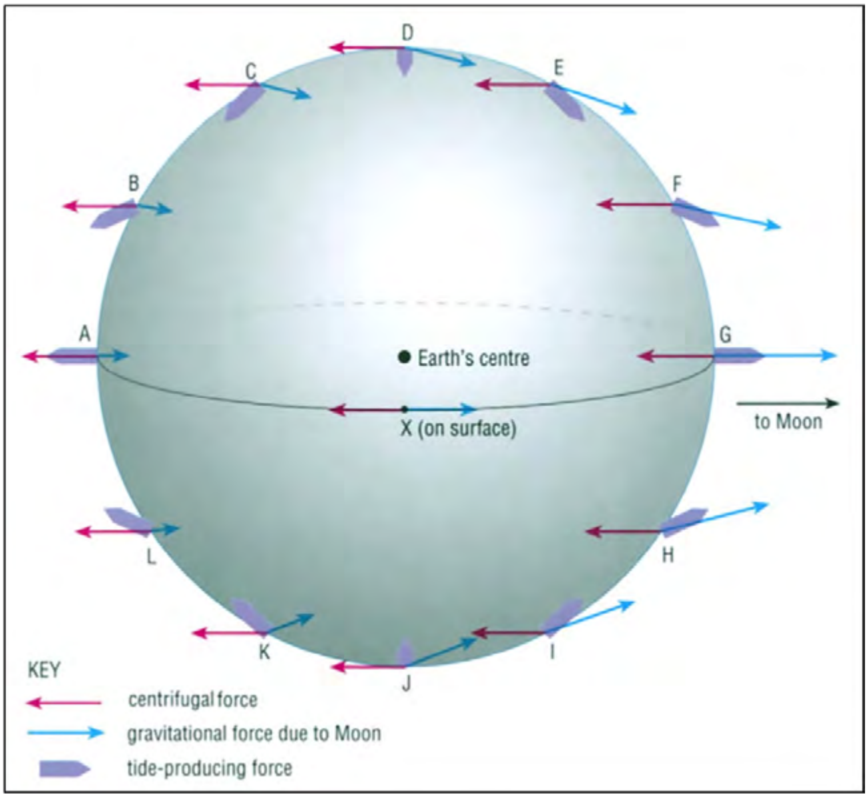

Source: Adapted from The Open University (1999).

Figure 1: Tide generating forces.

Analogously, the same interactions occur between the planet and the Sun, also causing the vertical movement of the oceans, but with less intensity. Thus, the effects generated by the influences of both celestial bodies interact sometimes in a constructive way, sometimes in a destructive way, as illustrated in Figure 2.

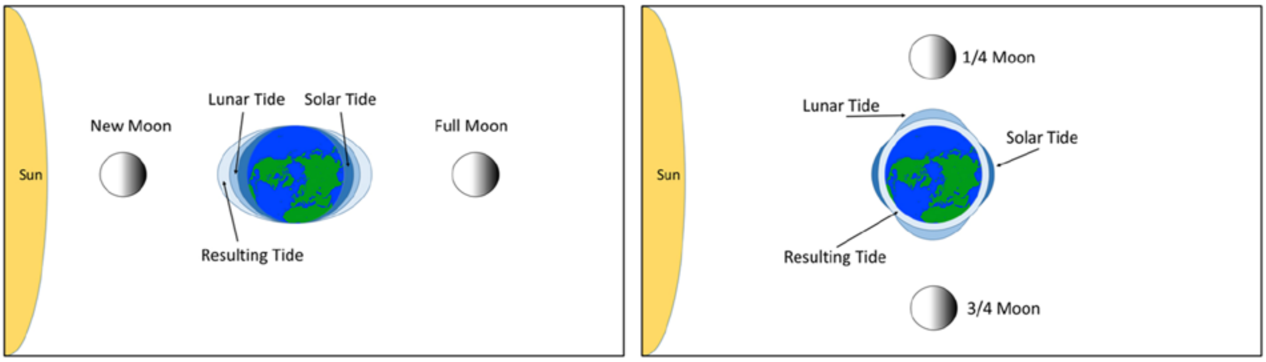

Source: Adapted from https://rwu.pressbooks.pub/webboceanography/chapter/11-1-tidal-forces/.

Figure 2: Interactions between influences from the Moon and the Sun on the Earth water masses: constructive interaction (left) and destructive interaction (right).

The constructive interaction is called spring tide and the destructive, neap tide. Thus, the vertical and periodic movement of water masses, generated by gravitational and centrifugal forces acting on the Earth and their respective interactions, basically describes the phenomenon of the tide. When the earth's rotation around its own axis is added, the basic tidal movement is completed as shown in Figure 3.

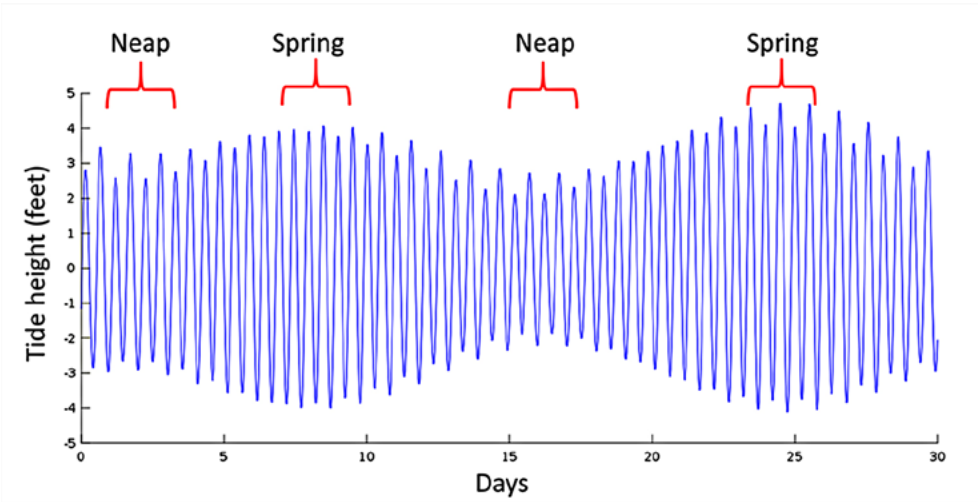

Source: https://rwu.pressbooks.pub/webboceanography/chapter/11-1-tidal-forces/.

Figure 3: Tidal movement.

In addition to these forces that effectively generate the tide, the phenomenon is also affected by other factors, such as the influence of land masses, the declinations of the Moon and the Sun, the elliptical orbits of the Moon and Earth, the friction between the ocean and the planet and the latitude of the place.

As basic characteristics, the tide describes a wave with one or two cycles in a mean lunar day, depending on the location where it is observed. Due to the low frequency of the phenomenon, the isolated recording of the tide movement depends on the removal of any transient or high frequency effects that affect both the sea surface and the measurement itself. In this way, digital data filters, more specifically low-pass filters, emerge as an important tool for the successful analysis of astronomical tides.

4.Data Filtering

A set of filters have been developed and presented in the literature. In this section we present the SMA filterand the wavelet compression method, tested and validated in this study.

1. Simple Moving Average (SMA) Filter

The SMA filter consists of a well-known and commonly applied attenuation method in signal processing (Smith, 1999). In general, a SMA Filter calculates the n-th value of the output sequence y[n] through the simple average of MT values of the input sequence x[n]. When it is calculated around the n-th value of the inserted sequence, the SMA Filter is formulated according to equations (1) and (2) (Vega, 2018).

$$y[n] = \frac{(x[n - M_P] + x[n - (M_P - 1)] + \ldots + x[n - (M_F - 1)] + x[n + M_F])}{M_T} \quad (1)$$

$$y[n] = \frac{1}{M_T} \sum_{k=-M_F}^{M_P} x[n - k] \quad (2)$$

Where: $M_T = (M_P + M_F + 1)$ and $\{M_P, M_F\} \in \mathbb{N}$

In general terms, the FMM results in the removal of high frequencies from the input signal (low-pass filter), depending exclusively on the value of MT, which consists of the sampling window of the filter. The reduction of high frequency signals occurs at a rate equal to the square root of MT.

2. Wavelet Compression

Wavelet compression or filtering is one of the applications of the Discrete Wavelet Transform (DWT). It is performed by using Orthogonal Filters Banks, in which the input signal is divided into different decomposition levels. These decomposition levels include many subbands, which contain coefficients representing the time-frequency characteristics of the original signal. In case of signal compression, this tool concentrates the energy of the input signal in a rather small number of specific wavelet coefficients maintaining a satisfactory quality in the resulting signal (Boukhobza et al., 2022).

This set of filters is determined by three parameters: the wavelet mother function, the number of vanishing moments of this function and the amount of decomposition levels. The wavelet mother functions are used to represent an input signal in time and space through the convolution between them. These can be symmetrical, orthogonal or both (biorthogonal) (Brassarote, 2020). Brassarote (2020) states that the most suitable wavelet functions for use in signal compression are the orthogonal ones, as they do not present redundancy in the representation of the source signal.

The number of vanishing moments is directly related to the smoothness of the function. According to Mallat (2009), the higher this value is, the smoother the representation of the input signal and the better the detection of singularities and transients will be.

The amount of decomposition levels is the number of frequency bands the signal is decomposed into. At each level, the upper-level information is decomposed into a high-frequency signal, which for the present study consists of noise, and a low-frequency signal, which represents the approximate or filtered signal at that level, as illustrated in Figure 4.

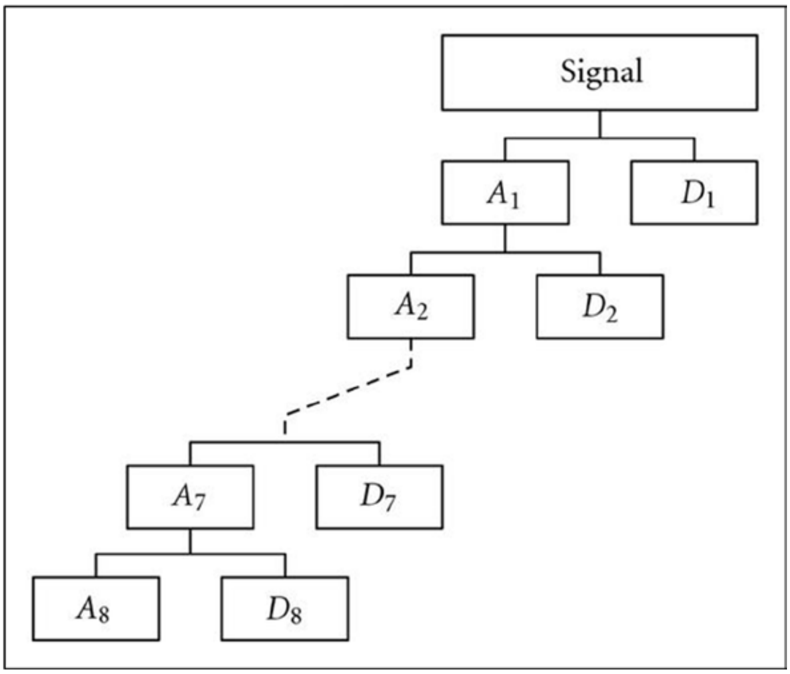

Source: https://www.hindawi.com/journals/ijrm/2009/265198/fig3/.

Figure 4: Representation of an example of Orthogonal Filters Banks with 8 decomposition levels.

5. Methodology

In the first step of the study, a dual frequency GNSS receiver C-NAV 3050, collecting data every 15 seconds, was fixed on the Brazilian Navy Hydrographic and Oceanographic Survey Ship Aspirante Moura, which remained moored in the wharf of the Directorate of Hydrography and Navigation, located in Niteroi, RJ. Between July 31st to August 11th, 2019, the vessel was subjected to the vertical variations of Guanabara Bay. At same time, a nearby tide gauge continuously collected sea level oscillations, which we considered as reference in our assessment. The geographic arrangement of the devices is illustrated in Figure 5.

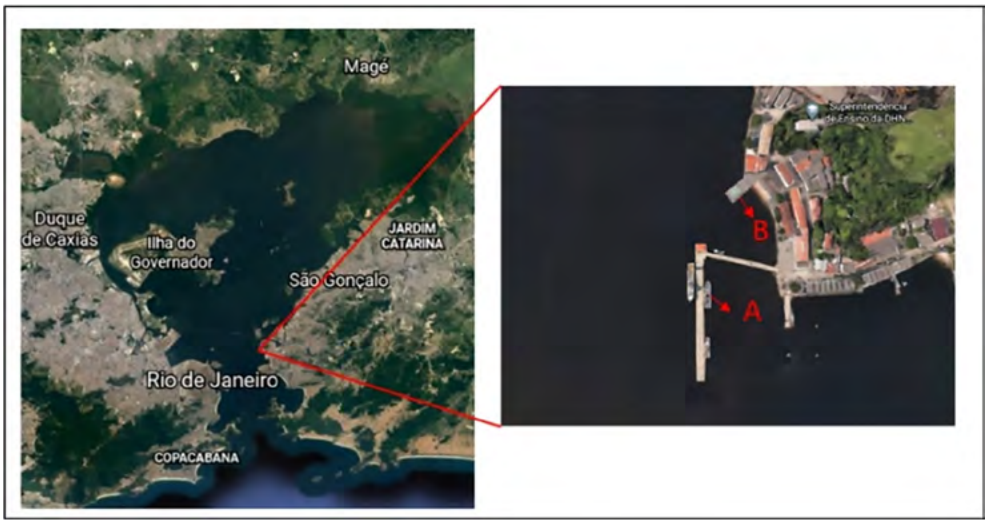

Source: The authors.

Figure 5: (left) Guanabara Bay area; (right) Vessel (Point A) and tide gauge (Point B) location.

For the positioning estimates, we employed the post-processing kinematic relative mode (PPK) using the Brazilian Network for Continuous Monitoring of the GNSS Systems (RBMC – Rede Brasileira de Monitoramento Contínuo) station in Niteroi (RJNI) as base. Figure 6 presents the baseline between both stations with de length of approximately 1.4 Km.

Source: The authors.

Figure 6: Relative positioning baseline.

We selected the RTKLIB application, version 2.4.2, (Takasu, 2013) to process our data. We used file to calibrate antenna phase center variations, precise ephemeris and, because of short baseline, it was not necessary to use neither clock correction files nor atmospheric models in the processing strategy. The applied configuration is detailed in Table 1.

Table 1: RTKLIB settings for the positioning processing.

GNSS Systems	GPS and GLONASS
Positioning Mode	Kinematic
Frequencies	L1 and L2
Filter Type	Combined
Elevation Mask	10°
Ionospheric Correction	OFF
Tropospheric Correction	OFF
Satellite Ephemerides / Clock	Precise
Integer Ambiguity Resolution Mode	Fix and Hold
Minimum Ratio to Fix Ambiguity	3

Among the configurations presented above, Filter Type and Integer Ambiguity Resolution Mode stand out. The former refers to the direction in time that the Kalman Filter is applied. The combined option allows to execute this filter in both directions, smoothing and combining solutions from forward and backward filters. Parajuli (2020) concluded that this choice results in better positioning accuracy compared to other options. Regarding the Integer Ambiguity Resolution Mode chosen, after the integer solution is checked in the validation test, the “Fix and Hold” mode include tight constraints to the integer solutions in the next update of the Kalman Filter. According to Takasu and Yasuda (2010), this mode tends to improve the initialization time and the fixing ratio in positioning.

Then, with the positioning results, the post-processing step started with the application of low-pass filters. We selected two types of data filters with different characteristics: the simple moving average (SMA) filter and the wavelet compression. Regarding the first one, we performed some analysis to find the most adequate window size for obtaining tidal heights from GNSS positioning data.

For the wavelet compression, we tested the orthogonal functions of Daubechies, Symmlets and Coifltes using as many vanishing moments as possible in each wavelet function tested to improve the resulting signal. Furthermore, we verified the ideal amount of decomposition levels for the application under analysis.

For the assessment of our results, we used as reference the tide gauge station, with all the data reduced by its respective average level to compare only the harmonic variation of the signals. We estimated the accuracy of the data in terms of the root-mean-squared error (RMSE) to verify the quality of each model generated by the filtered data, the standard deviation (σ) of the differences between the filtered and the reference data to analyze the dispersion of the results, and the determination index (R2) with the objective of checking the proximity of the modeled data with the reference dataset.

After all the tests and evaluations, we compared the best configuration of each type of data filter, allowing to reach the conclusion of which one would be the best choice. This last step considered, for each option, the quantitative characteristics, observed in the calculated statistical parameters, and qualitative ones, represented by the intrinsic particularities of the filters, such as complexity and computational needs for the implementation.

We performed all filter implementations as well as statistical computation and data plot using the MATLAB software, version 2023b (the Math Works Inc. 2023).

6. Results and Discussion

First, after processing the GNSS data, we compared the estimated time series of vertical components to the tide heights measured continuously by the tide gauge. Figure 7 presents both data graphically arranged, as well as the results of the statistical parameters referring to this comparison.

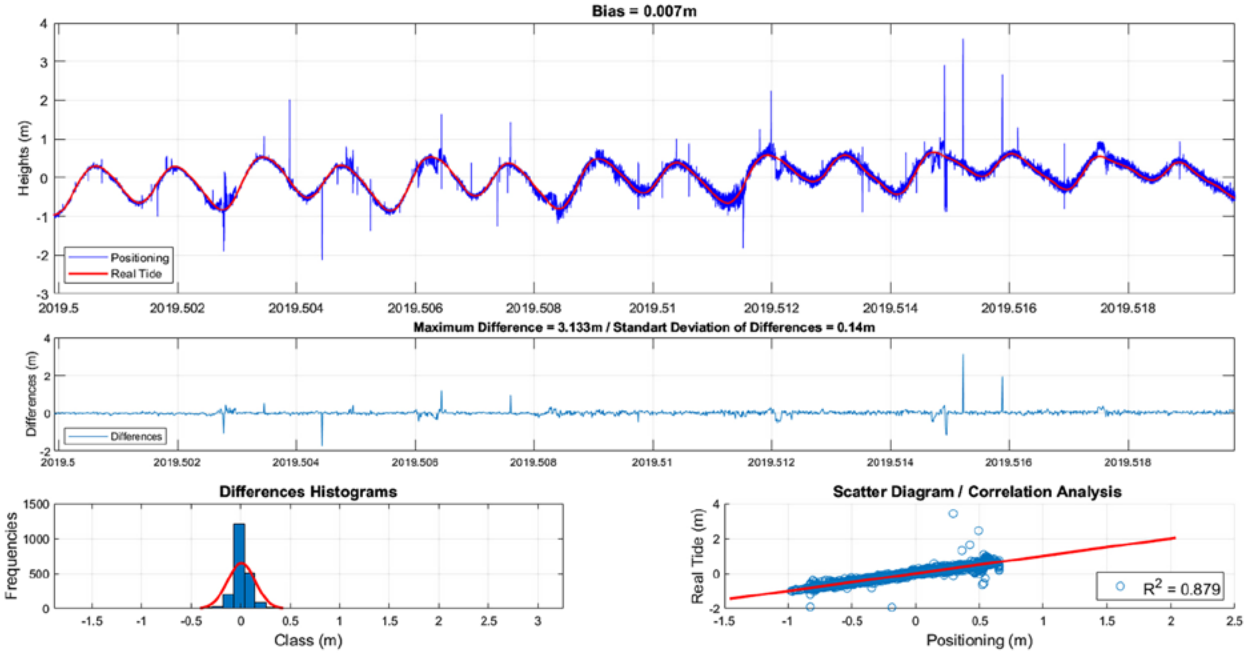

Source: The authors.

Figure 7: Comparative analysis between positioning data and tide gauge measurements.

As illustrated in Figure 7, it is observed that the signal represented by the vertical components of the positioning is composed of high frequency variations when compared to the tidal curve. In addition, the results of the statistical parameters demonstrate considerable dispersion and a correlation lower than 90% between the data. Thus, it can be verified, analytically, the need to apply data filters to better represent the tidal variations.

We initially applied the SMA filter and tested several window sizes to verify which one was closest to the reference data. Table 2 shows that the optimal window size was 2 hours (480 points), resulting in a bias of 0.005 m, standard deviation of differences of 0.045 m, and correlation index of 98.6%. The comparison between the data resulting from this configuration with the reference data is illustrated in Figure 8.

Table 2: Window Size selection.

Window Size	bias (m)	σ (m)	R^2 (%)
30min (120 points)	0.005	0.063	97.4
1h (240 points)	0.005	0.052	98.2
1h30min (360 points)	0.005	0.046	98.5
2h (480 points)	0.005	0.045	98.6
2h30min (600 points)	0.005	0.048	98.4

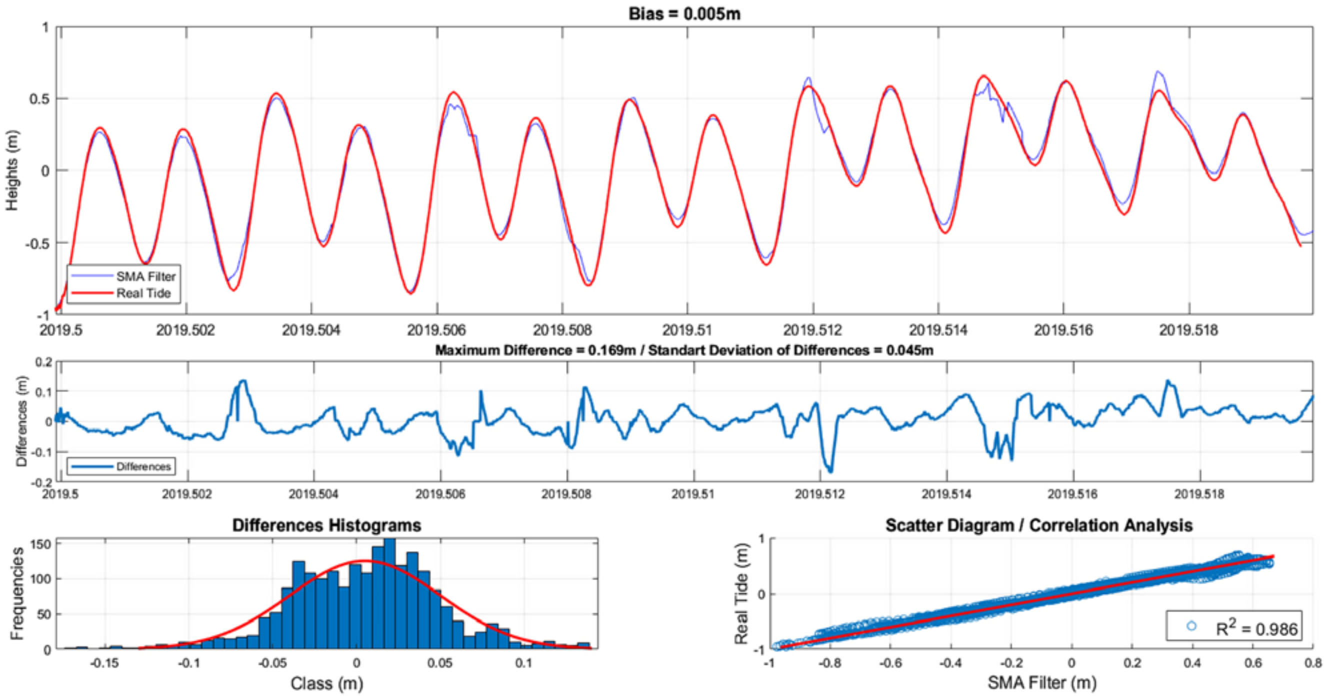

Figure 8: Comparative analysis between data filtered by SMA filter with window size of 2 hours (480 points) and tide gauge measurements.

After that, we applied and assessed the performance of orthogonal filter banks in our dataset. We used the Daubechies, Coiflets and Symlets wavelet functions. When analyzing the number of vanishing moments, we verified that quantities greater than 14 vanishing moments did not promote significant differences in terms of accuracy. Therefore, this was the amount used, except for the Coiflets functions, which the maximum value allowed by the MATLAB software was 5 vanishing moments. Thus, for each of these functions we only varied the number of levels of decomposition, with the statistical parameters being calculated in each test.

Table 3 shows that the best option tested was the one that used the Daubechies wavelet function with 14 vanishing moments and 9 levels of decomposition which resulted in a bias of 0.005 m, standard deviation of the differences of 0.040 m and determination index of 99.0 %. These results are graphically represented in Figure 9.

Table 3: Wavelet compression elements selection.

Wavelet Mother	Vanishing Moments	Levels of Decomposition	Bias (m)	σ (m)	R^2 (%)
Symmlets	14	8	0.005	0.053	98.1
		9	0.006	0.045	98.7
		10	0.007	0.067	96.9
Daubechies	14	8	0.005	0.054	98.1
		9	0.005	0.040	99.0
		10	0.006	0.066	97.1
Coiflets	14	8	0.005	0.053	98.2
		9	0.006	0.044	98.7
		10	0.008	0.068	96.9

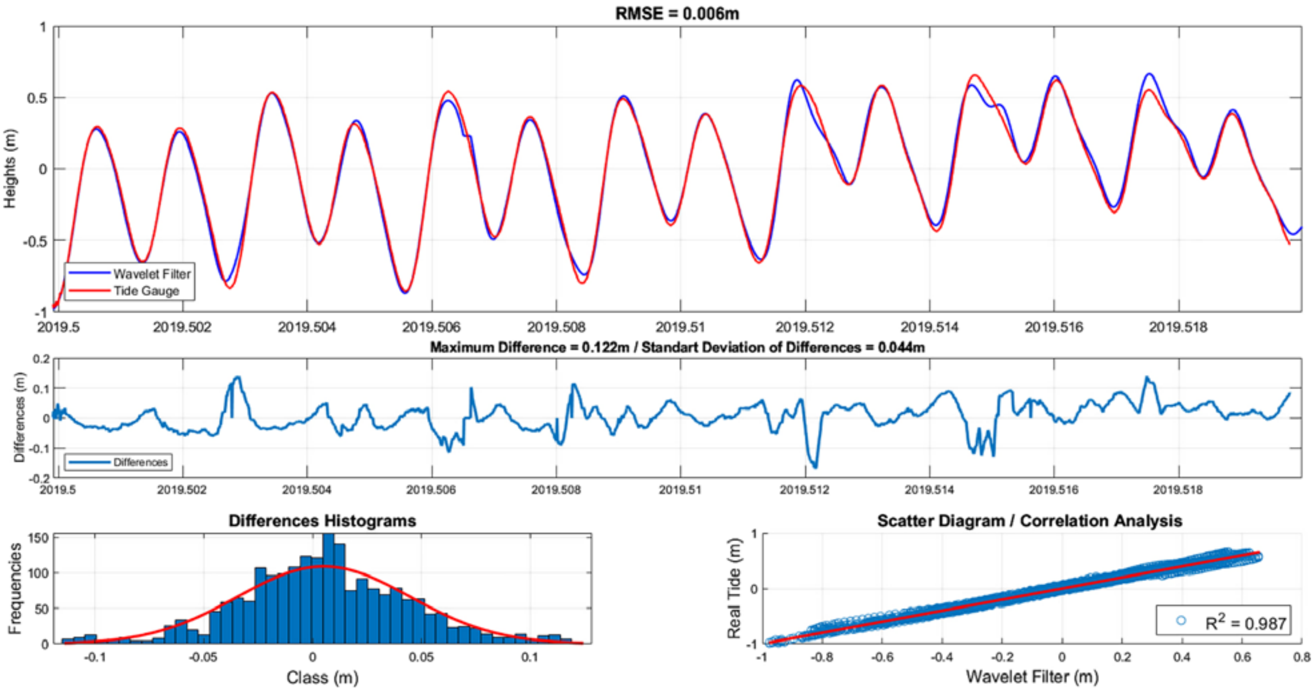

Figure 9: Comparative analysis between data filtered by Wavelet filter with best results and tide gauge measurements.

We then compared the filters that reached the closest approximation to the reference data to each other. Table 4 shows the statistical parameters calculated for these filter options. There is a notable equivalence between the best filters of each type, since both achieved similar statistical parameters with bias and σ in the order of a few millimeters and centimeters, respectively, and R2 close to 100%.

Table 4: Wavelet compression elements selection.

Filter Type	Bias (m)	σ (m)	R^2 (%)
Simple Moving Average Filter with size window of 2 hours (480 points)	0.005	0.045	98.6
Orthogonal Filters Bank with Daubechies wavelet mother function, 14 vanishing moments and 9 decomposition levels	0.005	0.040	99.0

Thus, we can observe that the filters generated quantitatively equivalent results. However, considering the characteristics of both, we can conclude that it would be more advantageous to use the SMA filter because its application is much simpler, depending on only one variable (sampling window) and, consequently, less computational resources.

4. Conclusion

This paper presents a quantitative and qualitative analysis of a methodology that aims to obtain ocean tides heights measurements from GNSS positioning. The data were collected during eight days by a receiver settled in a moored vessel located in Guanabara Bay, and we processed the observations in relative Kinematic mode in RTKLIB application.

For the tidal data to be properly extracted, we selected, applied and evaluated two data filters: the moving average filter and the wavelet compression to find out which would be the most advantageous option.

We verified that it was possible to obtain ocean tide data from GNSS observations with centimeter level accuracy when using both tested filters. This fact corroborates the results of previous studies, in addition it endorses the promising nature of using GNSS positioning for this specific purpose.

When comparing the best options for each type of filter, we verified the similarity of the calculated statistical parameters. and concluded that such filters produce quantitatively equivalent results. However, when analyzed qualitatively, the SMA filter presents itself as a more advantageous option due to its simplicity and ease of application.

Finally, in view of this possibility of indirect application of GNSS positioning, it is recommended to deepen this theme by setting up new tests and studies using other devices, such as buoys and different types of vessels, as well as employing other data filters, aim to apply this methodology in hydrographic surveys. With the consolidation of this knowledge, operational implementation of this technology in Brazilian nautical cartography will become feasible in the foreseeable future.

ACKNOWLEDGMENT

We acknowledge Brazilian Navy which, through Directorate of Hydrography and Navegation (DHN), provided the data used in this research.

AUTHOR´S CONTRIBUTION

Author 1: Conceptualization, literature review, methodology, data analysis, writing, editing; Author 2: Methodology, revision, writing, final approval; Author 3: Writing, revision; Author 4: Data Analysis.

REFERENCES

Bouin M. N. Ballu V. Calmant S. and Pelletier B. 2009. Improving resolution and accuracy of mean sea surface from kinematic GPS, Vanuatu Subduction Zone. Journal of Geodesy, 83(11), pp. 1017-1030.

Boukhobza A. Taleb N. Taleb-Ahmed A. and Bounoua A. 2022. Design of orthogonal filter banks using a multi-objective genetic algorithm for a speech coding scheme. Alexandria Engineering Journal, 61(10), pp. 7649-7657. [Online] DOI: https://doi.org/10.1016/j.aej.2022.01.017.

Brassarote G. O. N. 2020. Modelagem Funcional e Estocástica de Séries Temporais para a Atualização e Estimativa da Componente Altimétrica: Aplicação no Sistema Geodésico Brasileiro. PhD. São Paulo State University.

Chang C. C. Lee H. W. and Tsui I. F. 2011. Preliminary Test of Tide-Independent Bathymetric Measurement Based on GPS. Geomatics Research Australasis, 76, pp. 23-36. Available at <https://www.researchgate.net/publication/242720848_PRELIMINARY_TEST_OF_TIDE-INDEPENDENT_BATHYMETRIC_MEASUREMENT_BASED_ON_GPS> [acessed 29 July 2023].

Deloach S. R. 1996. GPS Tides: A Project to Determine Tidal Datums with The Global Positioning System (Technical report, no. 181). Fredericton: Dept. of Geodesy and Geomatics Engineering, UNB. Available through University of New Brunswick Library <https://gge.ext.unb.ca/Pubs/TR181.pdf> [acessed 29 July 2023].

Everett T. Taylor T. Lee D.K. and Akos D.M. 2022. Optimizing the Use of RTKLIB for Smartphone-Based GNSS Measurements. Sensors, 22(3825). [Online]. DOI: https://doi.org/10.3390/s22103825.

Franco A. S. 2009. Marés – Fundamentos, Análise e Previsão. 2nd ed. Niteroi: Diretoria de Hidrografia e Navegação.

Graps A. 1995. An introduction to wavelets. In: IEEE Computational Science and Engineering, 2(2), pp. 50-61. [Online]. DOI: https://doi.org/10.1109/99.388960.

International Hydrographic Organization (IHO). 2005. IHO Publication C-13: Manual on Hydrography. Monaco: International Hydrographic Bureau. Available at <https://iho.int/uploads/user/pubs/cb/c-13/C-13.pdf> [acessed 29 July 2023].

Ismail, N. A. S., Din, A. H. M., Hamden, M. H., Zulkifli, N. A., & Idris, K. M. 2023. Reduction of mean sea level depth based on tide gauge distance-dependent at Sungai Dinding, Lumut. The International Archives of the Photogrammetry, Remote Sensing and Spatial Information Sciences, 48(4/W6-2022), 167-177. [Online] Available: <https://isprs-archives.copernicus.org/articles/XLVIII-4-W6-2022/167/2023/ DOI: 10.5194/isprs-archives-XLVIII-4-W6-2022-167-2023> [acessed 06 Feb. 2024].

Langley R. B. Teunissen P. J. G. and Montenbruck O. 2017. Introduction to GNSS. In: Teunissen, P. J. G. and Montenbruck, O. ed. Springer Handbook of Global Navigation Satellite Systems. Berlin: Springer. Ch. 1.

Mallat S. G. 2009. A Wavelet Tour of Signal Processing. 3rd ed. Academic Press.

Mann D. 2007. GPS Techniques in Tidal Modeling. International Hydrography Review, 8(2), pp. 59-71. Available at <https://journals.lib.unb.ca/index.php/ihr/article/download/20791/23952> [acessed 29 July 2023].

Odijk D. 2017. Positioning Model. In: Teunissen, P. J. G. and Montenbruck, O. ed. Springer Handbook of Global Navigation Satellite Systems. Berlin: Springer. Ch. 21.

Odijk D and Wanninger L. 2017. Differential Positioning. In: Teunissen, P. J. G. and Montenbruck, O. ed. Springer Handbook of Global Navigation Satellite Systems. Berlin: Springer. Ch. 26.

Oliveira Jr. A. M. Arroyo-Suarez E. N. Ramos A. M. and Arentz M. F. R. 2010. Seabed mapping on an Earth Centered Earth Fixed (ECEF) geocentric reference frame. Cooperative validation with US Navy and Brazilian Navy in Guanabara Bay, Rio de Janeiro. Proceedings of 23rd International Technical Meeting of the Satellite Division of the Institute of Navigation (ION GNSS 2010), pp. 2064-2075. Available at <https://www.ion.org/publications/abstract.cfm?articleID=9320> [acessed 29 July 2023].

Parajuli B. 2020. Performance analysis of different positioning modes in RTKLIB Software. [Online] DOI: https://doi.org/10.13140/RG.2.2.20111.61608.

Smith S. W. 1999. The Scientist and Engineer's Guide to Digital Signal Processing. 2nd ed. San Diego: California Technical Publishing.

Takasu T. 2013. RTKLIB version 2.4.2. Available at <https://www.rtklib.com/rtklib.htm> [acessed 29 July 2023].

Takasu T.and Yasuda A. 2010. Kalman-Filter-Based Integer Ambiguity Resolution Strategy for Long-Baseline RTK with Ionosphere and Troposphere Estimation. Proceedings of 23rd International Technical Meeting of the Satellite Division of the Institute of Navigation (ION GNSS 2010), pp. 161-171. Available at <https://www.ion.org/publications/abstract.cfm?articleID=9143> [acessed 29 July 2023].

The Math Works, Inc. 2023. MATLAB. Version 2023b. Natick: The Math Works, Inc.

The Open University. 1999. Waves, Tides and Shallow Waters Processes. Butterworth-Heinemann. p. 50-86. ISBN 9780080363721. [Online] DOI: 10.1016/B978-008036372-1/50003-9.

US ARMY CORPS OF ENGINEERS (USACE). 2013. Engineer Manual No. 1110-2-1003: Hydrographic Surveying. Washington: Department of the Army. Available at <https://www.publications.usace.army.mil/USACE-Publications/Engineer-Manuals/u43544q/487964726F67726170686963/> [acessed 29 July 2023].

Vega A. S. 2018. Tutorial sobre Sistema de Média Móvel para Fundamentos de Processamento Digital de Sinais. Niteroi: Universidade Federal Fluminense. Available at <http://www.telecom.uff.br/~delavega/public/DSP/tutorial_SMM_dsp.pdf> [acessed 29 July 2023].